NAS-BERT: Task-Agnostic and Adaptive-Size BERT Compression with Neural Architecture Search

Jin Xu[1], Xu Tan[2], Renqian Luo[3], Kaitao Song[4], Jian Li[1], Tao Qin[2], Tie-Yan Liu[2]

[1]Institute for Interdisciplinary Information Sciences, Tsinghua University, China
[3]University of Science and Technology of China, [4]Nanjing University of science and technology, China
[2]Microsoft Research Asia, China

j-xu18@mails.tsinghua.edu.cn,xuta@microsoft.com,lrq@mail.ustc.edu.cn,kt.song@njust.edu.cn
lijian83@mail.tsinghua.edu.cn,{taoqin,tyliu}@microsoft.com

ABSTRACT

While pre-trained language models (e.g., BERT) have achieved impressive results on different natural language processing tasks, they have large numbers of parameters and suffer from big computational and memory costs, which make them difficult for real-world deployment. Therefore, model compression is necessary to reduce the computation and memory cost of pre-trained models. In this work, we aim to compress BERT and address the following two challenging practical issues: (1) The compression algorithm should be able to output multiple compressed models with different sizes and latencies, in order to support devices with different memory and latency limitations; (2) The algorithm should be downstream task agnostic, so that the compressed models are generally applicable for different downstream tasks. We leverage techniques in neural architecture search (NAS) and propose *NAS-BERT*, an efficient method for BERT compression. NAS-BERT trains a big supernet on a carefully designed search space containing a variety of architectures and outputs multiple compressed models with adaptive sizes and latency. Furthermore, the training of NAS-BERT is conducted on standard self-supervised pre-training tasks (e.g., masked language model) and does not depend on specific downstream tasks. Thus, the compressed models can be used across various downstream tasks. The technical challenge of NAS-BERT is that training a big supernet on the pre-training task is extremely costly. We employ several techniques including block-wise search, search space pruning, and performance approximation to improve search efficiency and accuracy. Extensive experiments on GLUE and SQuAD benchmark datasets demonstrate that NAS-BERT can find lightweight models with better accuracy than previous approaches, and can be directly applied to different downstream tasks with adaptive model sizes for different requirements of memory or latency.

CCS CONCEPTS

• **Computing methodologies → Natural language processing**; **Neural networks**.

KEYWORDS

BERT compression; task-agnostic; adaptive; neural architecture search; pre-training

1 INTRODUCTION

Pre-trained Transformer [45]-based language models like BERT [10], XLNet [54] and RoBERTa [30] have achieved impressive performance on a variety of downstream natural language processing tasks. These models are pre-trained on massive language corpus via self-supervised tasks to learn language representation and fine-tuned on specific downstream tasks. Despite their effectiveness, these models are quite expensive in terms of computation and memory cost, which makes them difficult for the deployment on different downstream tasks and various resource-restricted scenarios such as online servers, mobile phones, and embedded devices. Therefore, it is crucial to compress pre-trained models for practical deployment.

Recently, a variety of compression techniques have been adopted to compress pre-trained models, such as pruning [14, 33], weight factorization [24], quantization [38, 56], and knowledge distillation [5, 16, 18, 37, 40, 41]. Several existing works [5, 14, 24, 33, 37, 41, 43, 56] compress a large pre-trained model into a small or fast model with fixed size on the pre-training or fine-tuning stage and have achieved good compression efficiency and accuracy. However, from the perspective of practical deployment, a fixed-size model cannot be deployed in devices with different memory and latency constraints. For example, smaller models are preferred in embedded devices than in online servers, and faster inference speed is more critical in online services than in offline services. On the other hand, some previous methods [5, 16] compress the models on the fine-tuning stage for each specific downstream task. This can achieve good accuracy due to the dedicated design in each task. However, compressing the model for each task can be laborious and a compressed model for one task may not generalize well on another downstream task.

In this paper, we study the BERT compression in a different setting: the compressed models need to cover different sizes and latencies, in order to support devices with different kinds of memory and latency constraints; the compression is conducted on the pre-training stage so as to be downstream task-agnostic[1]. To this end, we propose NAS-BERT, which leverages neural architecture search (NAS) to automatically compress BERT models. We carefully design a search space that contains multi-head attention [45], separable convolution [20], feed-forward network and identity operations with different hidden sizes to find efficient models. In order to search models with adaptive sizes that satisfy diverse requirements of memory and latency constraints in different devices, we train a big supernet that contains all the candidate operations and architectures with weight sharing [1–3, 55]. In order to reduce the laborious compressing on each downstream task, we directly train the big supernet and get the compressed model on the pre-training task to make it applicable across different downstream tasks.

However, it is extremely expensive to directly perform architecture search in a big supernet on the heavy pre-training task. To improve the search efficiency and accuracy, we employ several techniques including block-wise search, search space pruning and performance approximation during the search process: (1) We adopt block-wise search [25] to divide the supernet into blocks so that the size of the search space can be reduced exponentially. To train each block, we leverage a pre-trained teacher model, divide the teacher model into blocks similarly, and use the input and output hidden states of the corresponding teacher block as paired data for training. (2) To further reduce the search cost of each block (even if block-wise search has greatly reduced the search space) due to the heavy burden of the pre-training task, we propose progressive shrinking to dynamically prune the search space according to the validation loss during training. To ensure that architectures with different sizes and latencies can be retained during the pruning process, we further divide all the architectures in each block into several bins according to their model sizes and perform progressive shrinking in each bin. (3) We obtain the compressed models under specific constraints of memory and latency by assembling the architectures in every block using performance approximation, which can reduce the cost in model selection.

We evaluate the models compressed by NAS-BERT on the GLUE [46] and SQuAD [35, 36] benchmark datasets. The results show that NAS-BERT can find lightweight models with various sizes from 5M to 60M with better accuracy than that achieved by previous work. Our contributions of NAS-BERT can be summarized as follows:

- We carefully design a search space that contains various architectures and different sizes, and apply NAS on the pre-training task to search for efficient lightweight models, which is able to deliver adaptive model sizes given different requirements of memory or latency and apply for different downstream tasks.

- We further apply block-wise search, progressive shrinking and performance approximation to reduce the huge search cost and improve the search accuracy.
- Experiments on the GLUE and SQuAD benchmark datasets demonstrate the effectiveness of NAS-BERT for model compression.

2 RELATED WORK

2.1 BERT Model Compression

Recently, compressing pre-trained models such as BERT [10] has been studied extensively and several techniques have been proposed such as knowledge distillation, pruning, weight factorization, quantization and so on. Existing works [5, 18, 24, 24, 37, 38, 40–43, 56, 56] aim to compress the pre-trained model into a fixed size of the model and have achieved a trade-off between the small parameter size (usually no more than 66M) and the good performance. However, these compressed models cannot be deployed in devices with different memory and latency constraints. Recent works [16] can deliver adaptive models for each specific downstream task and demonstrate the effectiveness of the task-oriented compression. For practical deployment, it can be laborious to compress models from each task. Other works [13] can produce compressed models on the pre-training stage that can directly generalize to downstream tasks, and allow for efficient pruning at inference time. However, they do not explore the potential of different architectures as in our work. Different from existing works, NAS-BERT aims for task-agnostic compression on the pre-training stage which eliminates the laborious compression for each specific downstream task, and carefully designs the search space which is capable to explore the potential of different architectures and deliver various models given diverse memory and latency requirements.

2.2 Neural Architecture Search for Efficient Models

Many works have leveraged NAS to search efficient models [2, 3, 17, 19, 26, 28, 29, 43, 47, 55]. Most of them focus on computer vision tasks and rely on specific designs on the convolutional layers (e.g., inverted bottleneck convolution [17] or elastic kernel size [2, 55]). Among them, once-for-all [2] and BigNAS [55] train a big supernet that contains all the candidate architectures and can get a specialized sub-network by selecting from the supernet to support various requirements (e.g., model size and latency). HAT [47] also trains a supernet with the adaptive widths and depths for machine translation tasks. Our proposed NAS-BERT also trains a big supernet. However, different from these methods, we target model compression for BERT at the pre-training stage, which is a more challenging task due to the large model size, search space and huge pre-training cost. In our preliminary experiments, directly applying the commonly used single path optimization [1, 2, 7, 15] in such a big supernet cannot even converge. Therefore, we introduce several techniques including block-wise search, progressive shrinking, and performance approximation to reduce the training cost, search space and improve search efficiency. Tsai et al. [43] apply one-shot NAS to search a faster Transformer but they cannot deliver multiple architectures to meet various constraints for deployment. Different from Tsai et al. [43], NAS-BERT 1) progressively shrinks the search

space to allocate more resources to promising architectures and thus can deliver various architectures without adding much computation; 2) designs bins in the shrinking algorithm to guarantee that we can search architectures to meet diverse memory and latency constraints. 3) explores novel architectures with convolution layer, multi-head attention, and feed-forward layer, and achieves better performance than previous works for BERT compression.

3 METHOD

In this section, we describe NAS-BERT, which conducts neural architecture search to find small, novel and accurate BERT models. To meet the requirements of deployment for different memory and latency constraints and across different downstream tasks, we 1) train a supernet with a novel search space that contains different sizes of models for various resource-restricted devices, and 2) directly search the models on the pre-training task to make them generalizable on different downstream tasks. The method can be divided into three steps: 1) search space design (Section 3.1); 2) supernet training (Section 3.2); 3) model selection (Section 3.3). Due to the huge cost to train the big supernet on the heavy pre-training task and select compressed models under specific constraints, we introduce several techniques including block-wise search, search space pruning and performance approximation in Section 3.2 and 3.3 to reduce the search space and improve the search efficiency.
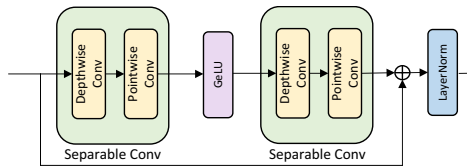
3.1 Search Space Design

A novel search space allows the potential of combinations of different operations, instead of simply stacking basic Transformer block (multi-head attention and feed-forward network) as in the original BERT model. We adopt the chain-structured search space [12], and construct an over-parameterized supernet $\mathcal{A}$ with L layers and each layer contains all candidate operations in $O = \{o_1, \cdots, o_C\}$, where C is the number of predefined candidate operations. Residual connection is applied to each layer by adding the input to the output. There are C^L possible paths (architectures) in the supernet, and a specific architecture $a = (a^1, \cdots, a^L)$ is a sub-net (path) in the supernet, where $a^l \in O$ is the operation in the l-th layer, as shown in Fig. 2 (a). We adopt weight sharing mechanism that is widely used in NAS [1, 2] for efficient training, where each architecture (path) shares the same set of operations in each layer.

We further describe each operation in O as follows: 1) Multi-head attention (MHA) and feed-forward network (FFN), which are the two basic operations in Transformer and are popular in pre-training models (in this way we can cover BERT model as a subnet in our supernet). 2) Separable convolution (SepConv), whose effectiveness and efficiency in natural language processing tasks have been demonstrated by previous work [20, 21]. 3) Identity operation, which can support architectures with the number of layers less than L. Identity operation is regarded as a placeholder in a candidate architecture and can be removed to obtain a shallower network. Apart from different types of operations, to allow adaptive model sizes, each operation can have different hidden sizes: {128, 192, 256, 384, 512}. In this way, architectures in the search space can be of different depths and widths. The complete candidate operation set O contains $(1 + 1 + 3) * 5 + 1 = 26$ operations, where the first product term represents the number of types of operations and

Table 1: Candidate operation set. For each type of operation including multi-head attention (MHA), feed-forward network (FFN) and separable convolution (SepConv) in each row, we list the number of heads in MHA and the size of the intermediate layer in FFN, and kernel size in SepConv under different hidden sizes.

Hidden Size	128	192	256	384	512
MHA	2 Heads	3 Heads	4 Heads	6 Heads	8 Heads
FFN	512	768	1024	1536	2048
SepConv	Kernel {3, 5, 7}				
Identity	Identity				

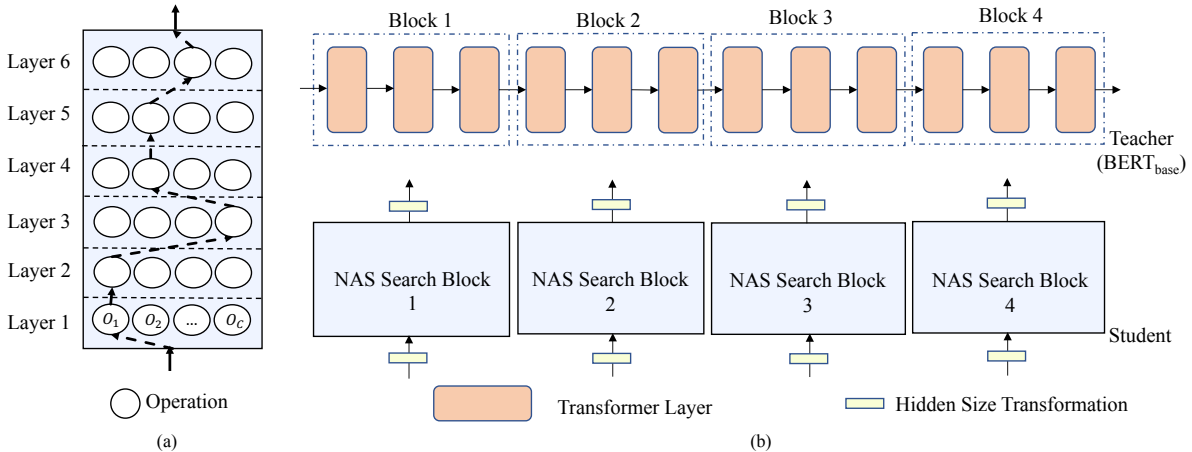**Figure 1: Structure of separable convolution.**

3 represents the SepConv with different kernel size {3, 5, 7}, the second product term represents that there are 5 different hidden sizes. We present 26 operations in Table 1 and structure of separable convolution in Fig. 1.

3.2 Supernet Training

3.2.1 Block-Wise Training with Knowledge Distillation. Directly training the whole supernet causes huge cost due to its large model size and huge search space. With limited computational resources (total training time, steps, etc.), the amortized training time of each architecture from the huge search space is insufficient for accurate evaluation [7, 27, 31]. Inspired by Li et al. [25], we adopt block-wise search to uniformly divide the supernet $\mathcal{A}$ into N blocks $(\mathcal{A}_1, \mathcal{A}_2, \cdots, \mathcal{A}_N)$ to reduce the search space and improve the efficiency. To train each block independently and effectively, knowledge distillation is applied with a pre-trained BERT model. The pre-trained BERT model (teacher) is divided into corresponding N blocks as in Fig. 2. The input and output hidden states of the corresponding block in the teacher model are used as the paired data to train the block in the supernet (student). Specifically, the n-th student block receives the output of the $(n-1)$-th teacher block as the input and is optimized to predict the output of the n-th teacher block with mean square loss

$$\mathcal{L}_n = ||f(\mathbf{Y}_{n-1}; \mathcal{A}_n) - \mathbf{Y}_n||_2^2, \tag{1}$$

where $f(\cdot; \mathcal{A}_n)$ is the mapping function of n-th block $\mathcal{A}_n$, $\mathbf{Y}_n$ is the output of the n-th block of the teacher model ($\mathbf{Y}_0$ is the output of the embedding layer of the teacher model). At each training step, we randomly sample an architecture from the search space following Bender et al. [1], Cai et al. [2], Guo et al. [15], which is memory-efficient due to the single path optimization. Different from Li et al. [25], we allow different hidden sizes and incorporate identity layer in each block to support elastic width and depth to derive models that meet various requirements. Besides, the search space within each block in our work is larger compared to Li et al.

Figure 2: (a) an architecture (path) in the supernet. (b) an illustration of block-wise distillation ($N = 4$ blocks). The supernet (student) and the pre-trained teacher model are divided into blocks respectively and each student block is trained to mimic the corresponding teacher block.

[25] (100x larger) which is much more sample in-efficient and requires more techniques (described in Section 3.2.2) to improve the training efficiency. Since the hidden sizes of the student block may be different from that in the teacher block, we cannot directly leverage the input and output hidden of the teacher block as the training data of the student block. To solve this problem, we use a learnable linear transformation layer at the input and output of the student block to transform each hidden size to match that of the teacher block, as shown in Fig. 2.

3.2.2 Progressive Shrinking. Although block-wise training can largely reduce the search space, the supernet still requires huge time for convergence due to the heavy pre-training task. To further improve the training effectiveness and efficiency, we propose to progressively shrink the search space in each block during training to allocate more training resources to more promising candidates [27, 32, 48]. However, simply pruning the architectures cannot ensure to obtain different sizes of models, since larger models in $\mathcal{A}_n$ are likely to be pruned on the early stage of training due to its difficulty of optimization [7, 27, 31] and smaller models are likely to be pruned at the late stage due to limited capacity. Therefore, we assign the architectures in $\mathcal{A}_n$ into different *bins* where each bin represents a short range of model sizes. Besides, we also apply latency constraints in each bin to avoid models accepted parameter size but large latency. Denote $p_b = \frac{b}{B} \cdot p(a^t)$ and $l_b = \frac{b}{B} \cdot l(a^t)$ as the maximum parameter size and latency for the b-th bin, where $p(\cdot)$ and $l(\cdot)$ calculate the parameter size and latency, a^t is the largest model in the search space and B is the number of bins. The architecture a in b-th bin should meet (1) $p_b > p(a) > p_{b-1}$ and (2) $l_b > l(a) > l_{b-1}$. Architectures that cannot satisfy the constraint of latency are removed.

Then we conduct the progressive shrinking algorithm in each bin at the end of each training epoch as follows: 1) **Sample** E architectures in each bin and get the validation losses on the dev set; 2) **Rank** the E architectures according to their validation losses in descending order; 3) **Remove** R architectures with the largest losses. The shrinking algorithm terminates when there are only m architectures left in the search space to avoid all the architectures

being deleted. The design of bins ensures the diversity of models when shrinking the search space, which makes it possible to select a model given diverse constraints at the model selection stage.

3.3 Model Selection

After the supernet training with progressive shrinking, each block contains $m * B$ possible architectures and the whole supernet (N blocks) contains $(m * B)^N$ complete architectures. The model selection procedure is as follows: 1) We build a large lookup table LT_{arch} with $(m * B)^N$ items, where each item contains the meta-information of a complete architecture: *(architecture, parameter, latency, loss)*. Since it is extremely time-consuming to measure the exact latency and loss for $(m * B)^N$ (e.g., 10^8 in our experiments) architectures, we use performance approximation to obtain the two values as described in the next paragraph. 2) For a given constraint of model size and inference latency, we select the top T architectures with low loss from LT_{arch} that meet the parameter and latency constraint. 3) We evaluate the validation loss of the top T complete architectures on the dev set and select the best one as the final compressed model.

Next we introduce the performance approximation of the latency and loss when building the lookup table LT_{arch}. We measure the latency of each candidate operation (just 26 in our design) on the target device and store in a lookup table LT_{lat} in advance, and then approximate the latency of an architecture $l(a)$ by $l(a) = \sum_{l=1}^{L} l(a^l)$ following Cai et al. [3], where $l(a^l)$ is from LT_{lat}. To approximate the loss of an architectures in LT_{arch}, we add up the block-wise distillation loss of the sub-architecture in each block on the dev set. Obtaining the dev loss of all sub-architectures in all blocks only involves $m * B * N$ evaluations.

4 EXPERIMENT

4.1 Experimental Setup

4.1.1 Supernet Training Setup. The supernet consists of $L = 24$ layers, which is consistent with BERT$_{base}$ [10] (BERT$_{base}$ has 12 Transformer layers with 24 sub-layers in total, since each Transformer

Table 2: Comparison of NAS-BERT models and hand-designed BERT models under different sizes (60M, 30M, 10M, 5M) on GLUE dev set. "PF" means pre-training and fine-tuning. "KD" means two-stage knowledge distillation. MNLI is reported in the matched set. Spearman correlation is reported for STS-B. Matthews correlation is reported for CoLA. Accuracy is reported for other tasks.

Setting	FLOPs	Speedup	MNLI	QQP	QNLI	CoLA	SST-2	STS-B	RTE	MRPC	AVG
$BERT_{60}$ + PF	1.3e10	2.2×	82.6	90.3	89.4	52.6	92.1	88.3	75.6	89.2	82.5
$NAS\text{-}BERT_{60}$ + PF	1.3e10	2.2×	83.0	90.9	90.8	53.8	92.3	88.7	76.7	88.9	**83.2**
$BERT_{60}$ + KD	1.3e10	2.2×	83.2	90.5	90.2	56.3	91.8	88.8	78.5	88.5	83.5
$NAS\text{-}BERT_{60}$ + KD	1.3e10	2.2×	84.1	91.0	91.3	58.1	92.1	89.4	79.2	88.5	**84.2**
$BERT_{30}$ + PF	7.1e9	3.6 ×	80.0	89.6	87.6	40.6	90.8	87.7	73.2	84.1	79.2
$NAS\text{-}BERT_{30}$ + PF	7.0e9	3.6 ×	80.4	90.0	87.8	48.1	90.3	87.3	71.4	84.9	**80.0**
$BERT_{30}$ + KD	7.1e9	3.6 ×	80.8	89.8	88.7	44.7	90.5	87.6	70.3	85.2	79.7
$NAS\text{-}BERT_{30}$ + KD	7.0e9	3.6 ×	81.0	90.2	88.4	48.7	90.5	87.6	71.8	84.6	**80.3**
$BERT_{10}$ + PF	2.3e9	9.1 ×	74.0	87.6	84.9	25.7	88.3	85.3	64.1	81.9	74.0
$NAS\text{-}BERT_{10}$ + PF	2.3e9	8.7 ×	76.0	88.4	86.3	27.8	88.6	84.3	68.7	81.5	**75.2**
$BERT_{10}$ + KD	2.3e9	9.1 ×	74.4	87.8	85.7	32.5	86.6	85.2	66.9	77.9	74.6
$NAS\text{-}BERT_{10}$ + KD	2.3e9	8.7 ×	76.4	88.5	86.3	34.0	88.6	84.8	66.6	79.1	**75.5**
$BERT_5$ + PF	8.6e8	20.7 ×	67.7	84.1	80.9	10.4	81.6	81.1	62.8	78.6	68.4
$NAS\text{-}BERT_5$ + PF	8.7e8	23.6 ×	74.2	85.7	83.9	19.6	84.9	82.8	67.0	80.0	**72.3**
$BERT_5$ + KD	8.6e8	20.7 ×	67.9	83.2	80.6	12.6	82.8	81.0	61.9	78.1	68.5
$NAS\text{-}BERT_5$ + KD	8.7e8	23.6 ×	74.4	85.8	84.9	19.8	87.3	83.0	66.6	79.6	**72.7**

layer has a MHA and FFN). We use a pre-trained $BERT_{base}$ [10] as the teacher model. The detailed configurations of the search space, teacher model training can be found in Appendix A.1 and A.2. The supernet is divided into $N = 4$ blocks and the search space in each block is divided into $B = 10$ bins. We first train the supernet for 3 epochs without progressive shrinking as a warm start, and then begin to shrink at the end of each later epoch. We randomly sample $E = 2000$ architectures for validation (evaluate all architectures when the number of architectures in search space is less than 2000) and perform the progressive shrinking to remove $R = E/2$ architectures for each bin as in Section 3.2.2. The shrinking process terminates when only $m = 10$ architectures are left in each bin in each block, and the training also ends. The supernet is trained on English Wikipedia plus BookCorpus (16GB size) using masked language modeling (MLM) following BERT[2] [10], with a batch size of 1024 sentences and each sentence consists of 512 tokens. The training costs 3 days on 32 NVIDIA P40 GPUs while training the $BERT_{base}$ teacher model costs 5 days. Other training configurations remain the same as the teacher model. We select $T = 100$ models from the table LT_{arch} on the model selection stage. In progressive shrinking, to reduce the time of evaluating all the candidates, we only evaluate on 5 batches rather than the whole dev set, which is accurate enough for the pruning according to our preliminary study.

4.1.2 Evaluation Setup on Downstream Tasks. We evaluate the effectiveness of NAS-BERT by pre-training the compressed models *from scratch* on the pre-training task and fine-tuning on the GLUE [46] and SQuAD benchmarks [35, 36]. The GLUE benchmark includes CoLA [50], SST-2 [39], MRPC [11], STS-B [4], QQP [6], MNLI [51], QNLI [36] and RTE [9]. Similar to previous methods [16, 37, 44, 49],

we also apply knowledge distillation and conduct it on two stages (i.e., pre-training and fine-tuning) as the default setting for evaluation. Considering the focus of our work is to compress pre-trained models with novel architectures instead of knowledge distillation, we only use prediction layer distillation and leave the various distillation techniques like layer-by-layer distillation, embedding layer distillation and attention matrix distillation [16, 18, 37, 41, 42, 49] that can further improve the performance as to future work. During fine-tuning on the GLUE benchmark, RTE, MRPC and STS-B are started from the model fine-tuned on MNLI following Liu et al. [30].

4.1.3 FLOPs and Latency. Following Clark et al. [8], we infer FLOPs with batch size of 1 and the sequence length of 128. The latency used in progressive shrinking and model selection is measured on Intel(R) Xeon(R) CPU E5-2690 v4 @ 2.60 GHz with 12 cores, but our method can be easily applied to other devices (e.g., mobile platforms, embedded devices) by using the lookup table LT_{lat} (described in Section 3.3) measured and built for the corresponding device. Following Sun et al. [41], Wang et al. [49], the inference time is evaluated on QNLI training set with batch size of 128 and the maximum sequence length of 128. The numbers reported are the average of 100 batches.

4.2 Results on the GLUE Datasets

While our NAS-BERT can compress models with adaptive sizes, we only show the results of compressed models with 60M, 30M, 10M and 5M parameter sizes (denoted as $NAS\text{-}BERT_{60}$, $NAS\text{-}BERT_{30}$, $NAS\text{-}BERT_{10}$ and $NAS\text{-}BERT_5$ respectively) on the GLUE benchmark due to the large evaluation cost, and list the model structures with different sizes in Table 10. We compare our NAS-BERT models with hand-designed BERT models under the same parameter size and latency (denoted as $BERT_{60}$, $BERT_{30}$, $BERT_{10}$ and $BERT_5$

---

[2]The next sentence tasks are not considered since previous work [30] have achieved good results without it.

Table 3: Results on the dev and test set of the GLUE benchmark. "*" means using data augmentation. The test set results are obtained from the official GLUE leaderboard.

Model	Params	MNLI	QQP	QNLI	CoLA	SST-2	STS-B	RTE	MRPC	AVG
dev set										
Teacher	110M	85.2	91.0	91.3	61.0	92.9	90.3	76.0	87.7	84.4
DistilBERT	66M	82.2	88.5	89.2	51.3	91.3	86.9	59.9	87.5	79.6
MiniLM	66M	84.0	91.0	91.0	49.2	92.0	-	71.5	88.4	-
BERT-of-Theseus	66M	82.3	89.6	89.5	51.1	91.5	88.7	68.2	-	-
PD-BERT	66M	82.5	90.7	89.4	-	91.1	-	66.7	84.9	-
DynaBERT*	60M	84.2	**91.2**	91.5	56.8	92.7	89.2	72.2	84.1	82.7
NAS-BERT	60M	84.1	91.0	91.3	58.1	92.1	89.4	79.2	88.5	84.2
NAS-BERT*	60M	**84.8**	**91.2**	**91.9**	**58.7**	**93.1**	**89.9**	**79.8**	**88.9**	**84.8**
test set										
Teacher	110M	84.8	89.0	91.7	57.1	94.1	88.0	71.0	84.1	82.5
BERT-of-Theseus	66M	82.4	**89.3**	89.6	47.8	92.2	84.1	66.2	83.2	79.4
PD-BERT	66M	82.8	88.5	88.9	-	91.8	-	65.3	81.7	-
BERT-PKD	66M	81.5	88.9	89.0	-	92.0	-	65.5	79.9	-
TinyBERT*	66M	**84.6**	89.1	90.4	**51.1**	**93.1**	83.7	70.0	82.6	80.6
NAS-BERT	60M	83.5	88.9	90.9	48.4	92.9	86.1	**73.7**	84.5	81.1
NAS-BERT*	60M	84.1	88.8	**91.2**	50.5	92.6	**86.9**	72.7	**86.4**	**81.7**

respectively). We follow several principles when manually designing the BERT models: 1) The size of the embedding layer is the same as that of the corresponding NAS-BERT model; 2) We use the original BERT structure (MHA plus FFN) and keep the parameter, latency, depth and width as close as possible to the corresponding NAS-BERT model. The baseline BERT models in Table 2 are: $BERT_{60}$ (L=10, H=512, A=8), $BERT_{30}$ (L=6, H=512, A=8), $BERT_{10}$ (L=6, H=256, A=4) and $BERT_5$ (L=6, H=128, A=2) where L is the number of layers, H is the hidden size, and A is the number of attention heads. To demonstrate the advantages of architectures searched by NAS-BERT, the comparisons are evaluated in two settings: 1) only with pre-training and fine-tuning (PF), and 2) pre-training and fine-tuning with two-stage knowledge distillation (KD). The results are shown in Table 2, from which we can see that NAS-BERT outperforms hand-designed BERT baseline across almost all the tasks under various model sizes. Especially, the smaller the model size is, the larger gap can be observed (e.g., $NAS-BERT_5$ vs. $BERT_5$). The results show that NAS-BERT can search for efficient lightweight models that are better than Transformer based models.

4.3 Comparison with Previous Work

4.3.1 Comparison in commonly used model size . Next, we compare the effectiveness of our NAS-BERT to previous methods on BERT compression. Since they usually compress BERT into a model size of about 66M or 60M, we use our $NAS-BERT_{60}$ for comparison. We mainly compare our NAS-BERT with methods whose teacher model is $BERT_{base}$ for a fair comparison including 1) DistilBERT [37], which uses knowledge distillation on the pre-training stage; 2) BERT-PKD [41], which distills the knowledge from the intermediate layers and the final output logits on the pre-training stage; 3) BERT-of-Theseus [53], which uses module replacement for compression; 4) MiniLM [49], which transfers the knowledge from the

self-attention module; 5) PD-BERT [44], which distills the knowledge from the target domain in BERT training; 6) DynaBERT [16], which uses network rewiring to adjust width and depth of BERT for each downstream task. 7) TinyBERT [18], which leverage embedding layer, hidden layer, and attention matrix distillation to mimic the teacher model at both the pre-training and fine-tuning stages. The comparison of their teacher models is presented in Table 9. We do not compare with MobileBERT [42] since it uses a teacher model with much higher accuracy than the commonly used $BERT_{base}$ (nearly matches to the accuracy of $BERT_{large}$), and the pre-training computations of its student model (4096 batch size * 740,000 steps) is significantly larger than that of other method [10, 37, 41] and NAS-BERT (2048 batch size * 125,000 steps). Nevertheless, we will compare with MobileBERT in future work. To make comparison with DynaBERT and TinyBERT, we also use their data augmentation [16, 18] on downstream tasks. Table 3 reports the results on the dev and test set of the GLUE benchmark. Without data augmentation, NAS-BERT achieves better results on nearly all the tasks compared to previous work. Further, with data augmentation, NAS-BERT outperforms DynaBERT and TinyBERT. Different from these methods that leverage advanced knowledge distillation techniques in pre-training and/or fine-tuning, NAS-BERT mainly takes advantage of architectures and achieves better accuracy, which demonstrates the advantages of NAS-BERT in model compression.

4.3.2 Comparison in extremely small model size. Compressing the pre-training model into an extremely small model with good accuracy is challenging. Previous works usually compress the model at the fine-tuning stage for each specific task with sophisticated techniques. For example, AdaBERT [5] searches a task-specific architecture (6M - 10M) for each task, and introduces the special distillation techniques (e.g., using probe classifiers to hierarchically decompose the task-useful knowledge from the teacher model) and
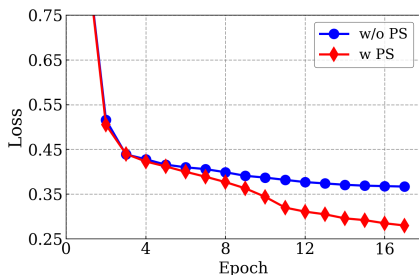
data augmentations to boost the performance. To show the effectiveness of our searched architecture in the extremely small size itself, we compare NAS-BERT with AdaBERT without sophisticated techniques. Specifically, we do not use two-stage distillation and data augmentation for NAS-BERT$_5$, and do not use data augmentation and probe classifiers for AdaBERT. As shown in Table 4, we can find that NAS-BERT$_5$ (with an only 5M model size) can greatly improve upon AdaBERT (with slightly larger model size) by 1.9%, 2.8% and 10.3% (absolute differences) on QNLI, MRPC, and RTE.

Table 4: Comparison in extremely small model size.

Setting	QNLI/Params	MRPC/Params	RTE/Params
AdaBERT	82.0/7.9M	77.2/7.5M	56.7/8.6M
NAS-BERT	83.9/5.0M	80.0/5.0M	67.0/5.0M

4.4 Ablation Study

4.4.1 Ablation Study on Progressive Shrinking. To verify the effectiveness of progressive shrinking (PS), we train the supernet with the same number of training epochs but without progressive shrinking. We follow the same procedure in NAS-BERT for model selection and final evaluation on downstream tasks. Due to the huge evaluation cost during the model selection on the whole search space without progressive shrinking, it costs 50 hours (evaluation cost on the shrinked search space only takes 5 minutes since there are only 10 architectures remaining in each bin in each block). The results are shown in Table 5. It can be seen that NAS-BERT with progressive shrinking searches better architectures, with less total search time.

Figure 3: Loss curve of supernet training. Progressive shrinking starts at the epoch 4.

We further show the training loss curve in Fig. 3. It can be seen that the superset without progressive shrinking suffers from slow convergence. The huge number of architectures in the supernet need long time for sufficient training. Given a fixed budget of training time, progressive shrinking can ensure the promising architectures to be trained with more resources and result in more accurate evaluation, and thus better architectures can be selected. On the contrary, without progressive shrinking, the amortized training time of each architecture is insufficient, resulting in inaccurate evaluation and model selection.

4.4.2 Different Progressive Shrinking Approaches. Instead of pruning architectures (paths) from the search space, we can also prune operations (nodes) from the supernet [32, 34] in progressive shrinking. From the perspective of supernet, the former is to remove paths

and the latter is to remove nodes from the supernet. To evaluate the performance of operations (nodes) in supernet, at the end of each training epoch, we evaluate the architectures on the dev set and prune the search space according to the performance (validation loss) of operations. The validation loss of the operation o_i in l-layer is estimated by the mean validation losses of all the architectures whose operation in the l-th layer $a^l = o_i$. The shrinking algorithm proceeds as follows:

- Sample E architectures and get the validation losses on the dev set.
- Rank operations according to their mean validation losses in descending order.
- Prune operations with the largest losses from the supernet repeatedly until removing R (R is a hyper-parameter to control the speed of pruning) of the architectures in the search space.

The shrinking algorithm performs at the end of each training epoch, and terminates when only $m = 10$ architectures are left in each bin in each block, and the training also ends. For the fair comparison, we set $m = 10$ and $E = 1000$, which are same as settings in Section 4.1. At the end of each epoch, we perform this algorithm to remove $R = 30\%$ architectures for each bin. In this way, the algorithm terminates at the same epoch as that in Section 3.2.2. At the end of each training epoch, we evaluate the architectures on the dev set and prune the search space according to the performance of *operations*. As shown in Table 6, pruning architectures in progressive shrinking achieves better results.

4.4.3 Ablation study of two-stage distillation. We further study the effectiveness of NAS-BERT by removing the distillation on pre-training or fine-tuning stage: 1) only using the distillation on the pre-training stage; 2) only using the distillation on the fine-tuning stage. The results are presented in Table 7. We can find that 1) NAS-BERT consistently outperforms the BERT baseline in different settings; 2) distillation on either pre-training or fine-tuning stage can improve the accuracy, and two-stage distillation can further get better accuracy; 3) when removing the distillation at the fine-tuning stage, this setting becomes fully task-agnostic (the model is compressed in pre-training stage, and only needs fine-tuning on each downstream task). We can find that NAS-BERT can still achieve a score of 83.5 on average, which outperforms the previous works in Table 3. These results demonstrate that our searched architectures are effective regardless of the specific distillation settings. NAS-BERT can still achieve good results when removing distillation on the fine-tuning stage.

4.5 Results on the SQuAD Datasets

We further evaluate our method on the SQuAD v1.1 [36] and SQuAD v2.0 [35], which require to predict the answer span based on the given question and passage. For SQuAD v1.1, each question has the corresponding answer based on the given passage. And for SQuAD v2.0, some questions do not have the corresponding answer. Following previous practices [30], we add an additional binary classification layer to predict whether the answer exists for SQuAD v2.0. The results are shown in Table 8. We can find that our NAS-BERT outperforms previous works on both SQuAD v1.1 and v2.0.

Table 5: The results of NAS-BERT with and without progressive shrinking (PS) on NAS-BERT$_{60}$.

Setting	MNLI	QQP	QNLI	CoLA	SST-2	STS-B	RTE	MRPC	AVG
w/o PS	83.5	90.6	90.8	55.5	92.0	88.1	77.4	86.5	83.1
w PS	84.1	91.0	91.3	58.1	92.1	89.4	79.2	88.5	**84.2**

Table 6: The results of different progressive shrinking approaches on NAS-BERT$_{60}$. PS-arch and PS-op denote pruning architectures and operations in progressive shrinking.

Setting	MNLI	QQP	QNLI	CoLA	SST-2	STS-B	RTE	MRPC	AVG
PS-arch	84.1	91.0	91.3	58.1	92.1	89.4	79.2	88.5	**84.2**
PS-op	83.8	91.0	90.2	54.5	92.0	88.8	75.6	86.1	82.8

Table 7: Ablation study of two-stage knowledge distillation. "PD" or "FD" means to add knowledge distillation on the pre-training or the fine-tuning stage.

Setting	PD	FD	MNLI	QQP	QNLI	CoLA	SST-2	STS-B	RTE	MRPC	AVG
BERT$_{60}$	✓	✓	83.2	90.5	90.2	56.3	91.8	88.8	78.5	88.5	83.5
NAS-BERT$_{60}$	✓	✓	84.1	91.0	91.3	58.1	92.1	89.4	79.2	88.5	**84.2**
BERT$_{60}$	✓		83.2	90.3	89.5	55.0	91.6	88.6	77.8	87.3	82.9
NAS-BERT$_{60}$	✓		83.3	90.9	91.3	55.6	92.0	88.6	78.5	87.5	**83.5**
BERT$_{60}$		✓	83.1	90.4	90.4	54.3	91.2	88.7	75.6	87.0	82.6
NAS-BERT$_{60}$		✓	83.7	90.8	91.0	54.2	92.1	89.4	76.0	87.5	**83.1**

Table 8: Results on the dev set of the SQuAD v1.1 and SQuAD v2.0 dataset. MiniLM† means that MiniLM is trained with batch size 1024 and 400,000 steps. Thus we train the NAS-BERT† with batch size 2048 and 200,000 steps for a fair comparison.

Model	Params	SQuAD v1.1		SQuAD v2.0	
		EM	F1	EM	F1
Teacher	110M	81.8	88.9	74.5	77.9
DistilBERT	66M	79.1	86.9	-	-
BERT-PKD	66M	77.1	85.3	66.3	69.8
MiniLM†	66M	-	-	-	76.4
TinyBERT	66M	79.7	87.5	69.9	73.4
NAS-BERT	60M	80.5	88.0	73.2	76.3
NAS-BERT†	60M	**81.2**	**88.4**	**73.9**	**77.1**

5 CONCLUSION

In this paper, we propose NAS-BERT, which leverages neural architecture search (NAS) to compress BERT models. We carefully design a search space with different operations associated with different hidden sizes, to explore the potential of diverse architectures and derive models with adaptive sizes according to the memory and latency requirements of different devices. The compression is conducted on the pre-training stage and is downstream task agnostic, where the compressed models can be applicable for different downstream tasks. Experiments on the GLUE and SQuAD benchmark datasets demonstrate the effectiveness of our proposed NAS-BERT compared with both hand-designed BERT baselines and previous works on BERT compression. For future work, we will explore more advanced search space and NAS methods to achieve better performance.

6 ACKNOWLEDGEMENTS

REFERENCES

[1] Gabriel Bender, Pieter-Jan Kindermans, Barret Zoph, Vijay Vasudevan, and Quoc Le. 2018. Understanding and simplifying one-shot architecture search. In *International Conference on Machine Learning*. 550–559.

[2] Han Cai, Chuang Gan, Tianzhe Wang, Zhekai Zhang, and Song Han. 2019. Once-for-All: Train One Network and Specialize it for Efficient Deployment. In *International Conference on Learning Representations*.

[3] Han Cai, Ligeng Zhu, and Song Han. 2018. ProxylessNAS: Direct Neural Architecture Search on Target Task and Hardware. In *International Conference on Learning Representations*.

[4] Daniel Cer, Mona Diab, Eneko Agirre, Iñigo Lopez-Gazpio, and Lucia Specia. 2017. SemEval-2017 Task 1: Semantic Textual Similarity Multilingual and Crosslingual Focused Evaluation. In *Proceedings of the 11th International Workshop on Semantic Evaluation (SemEval-2017)*. 1–14.

[5] Daoyuan Chen, Yaliang Li, Minghui Qiu, Zhen Wang, Bofang Li, Bolin Ding, Hongbo Deng, Jun Huang, Wei Lin, and Jingren Zhou. 2020. AdaBERT: Task-Adaptive BERT Compression with Differentiable Neural Architecture Search. In *Proceedings of the Twenty-Ninth International Joint Conference on Artificial Intelligence, IJCAI-20*, Christian Bessiere (Ed.). International Joint Conferences on Artificial Intelligence Organization, 2463–2469. https://doi.org/10.24963/ijcai.2020/341 Main track.

[6] Zihan Chen, Hongbo Zhang, Xiaoji Zhang, and Leqi Zhao. 2018. Quora question pairs.

[7] Xiangxiang Chu, Bo Zhang, Ruijun Xu, and Jixiang Li. 2019. Fairnas: Rethinking evaluation fairness of weight sharing neural architecture search. *arXiv preprint arXiv:1907.01845* (2019).

[8] Kevin Clark, Minh-Thang Luong, Quoc V Le, and Christopher D Manning. 2019. ELECTRA: Pre-training Text Encoders as Discriminators Rather Than Generators. In *International Conference on Learning Representations*.

[9] Ido Dagan, Oren Glickman, and Bernardo Magnini. 2006. The PASCAL Recognising Textual Entailment Challenge. In *Machine Learning Challenges. Evaluating Predictive Uncertainty, Visual Object Classification, and Recognising Tectual Entailment*. 177–190.

[10] Jacob Devlin, Ming-Wei Chang, Kenton Lee, and Kristina Toutanova. 2019. BERT: Pre-training of Deep Bidirectional Transformers for Language Understanding. In *Proceedings of the 2019 Conference of the North American Chapter of the Association for Computational Linguistics: Human Language Technologies, Volume 1 (Long and Short Papers)*. Association for Computational Linguistics, Minneapolis, Minnesota, 4171–4186. https://doi.org/10.18653/v1/N19-1423

[11] William B. Dolan and Chris Brockett. 2005. Automatically Constructing a Corpus of Sentential Paraphrases. In *Proceedings of the Third International Workshop on Paraphrasing (IWP2005)*.

[12] Thomas Elsken, Jan Hendrik Metzen, and Frank Hutter. 2018. Neural architecture search: A survey. *arXiv preprint arXiv:1808.05377* (2018).

[13] Angela Fan, Edouard Grave, and Armand Joulin. 2019. Reducing Transformer Depth on Demand with Structured Dropout. In *International Conference on Learning Representations*.

[14] Mitchell Gordon, Kevin Duh, and Nicholas Andrews. 2020. Compressing BERT: Studying the Effects of Weight Pruning on Transfer Learning. In *Proceedings of the 5th Workshop on Representation Learning for NLP*. 143–155.

[15] Zichao Guo, Xiangyu Zhang, Haoyuan Mu, Wen Heng, Zechun Liu, Yichen Wei, and Jian Sun. 2020. Single path one-shot neural architecture search with uniform sampling. In *European Conference on Computer Vision*. Springer, 544–560.

[16] Lu Hou, Zhiqi Huang, Lifeng Shang, Xin Jiang, Xiao Chen, and Qun Liu. 2020. DynaBERT: Dynamic BERT with Adaptive Width and Depth. *Advances in Neural Information Processing Systems* 33 (2020).

[17] Andrew Howard, Mark Sandler, Grace Chu, Liang-Chieh Chen, Bo Chen, Mingxing Tan, Weijun Wang, Yukun Zhu, Ruoming Pang, Vijay Vasudevan, et al. 2019. Searching for mobilenetv3. In *Proceedings of the IEEE International Conference on Computer Vision*. 1314–1324.

[18] Xiaoqi Jiao, Yichun Yin, Lifeng Shang, Xin Jiang, Xiao Chen, Linlin Li, Fang Wang, and Qun Liu. 2020. TinyBERT: Distilling BERT for Natural Language Understanding. In *Proceedings of the 2020 Conference on Empirical Methods in Natural Language Processing: Findings*. 4163–4174.

[19] Haifeng Jin, Qingquan Song, and Xia Hu. 2019. Auto-keras: An efficient neural architecture search system. In *Proceedings of the 25th ACM SIGKDD International Conference on Knowledge Discovery & Data Mining*. 1946–1956.

[20] Lukasz Kaiser, Aidan N Gomez, and Francois Chollet. 2018. Depthwise Separable Convolutions for Neural Machine Translation. In *International Conference on Learning Representations*.

[21] Antonios Karatzoglou, Nikolai Schnell, and Michael Beigl. 2020. Applying depthwise separable and multi-channel convolutional neural networks of varied kernel size on semantic trajectories. *Neural Computing and Applications* 32, 11 (2020), 6685–6698.

[22] Diederik P Kingma and Jimmy Ba. 2015. Adam: A Method for Stochastic Optimization. In *ICLR (Poster)*.

[23] Guillaume Lample, Alexandre Sablayrolles, Marc'Aurelio Ranzato, Ludovic Denoyer, and Hervé Jégou. 2019. Large memory layers with product keys. In *Advances in Neural Information Processing Systems*. 8548–8559.

[24] Zhenzhong Lan, Mingda Chen, Sebastian Goodman, Kevin Gimpel, Piyush Sharma, and Radu Soricut. 2019. ALBERT: A Lite BERT for Self-supervised Learning of Language Representations. In *International Conference on Learning Representations*.

[25] Changlin Li, Jiefeng Peng, Liuchun Yuan, Guangrun Wang, Xiaodan Liang, Liang Lin, and Xiaojun Chang. 2020. Block-wisely Supervised Neural Architecture Search with Knowledge Distillation. In *Proceedings of the IEEE/CVF Conference on Computer Vision and Pattern Recognition*. 1989–1998.

[26] Ting Li, Junbo Zhang, Kainan Bao, Yuxuan Liang, Yexin Li, and Yu Zheng. 2020. Autost: Efficient neural architecture search for spatio-temporal prediction. In *Proceedings of the 26th ACM SIGKDD International Conference on Knowledge Discovery & Data Mining*. 794–802.

[27] Xiang Li, Chen Lin, Chuming Li, Ming Sun, Wei Wu, Junjie Yan, and Wanli Ouyang. 2020. Improving one-shot nas by suppressing the posterior fading. In *Proceedings of the IEEE/CVF Conference on Computer Vision and Pattern Recognition*. 13836–13845.

[28] Bill Yuchen Lin, Ying Sheng, Nguyen Vo, and Sandeep Tata. 2020. FreeDOM: A Transferable Neural Architecture for Structured Information Extraction on Web Documents. In *Proceedings of the 26th ACM SIGKDD International Conference on Knowledge Discovery & Data Mining*. 1092–1102.

[29] Hanxiao Liu, Karen Simonyan, and Yiming Yang. 2018. DARTS: Differentiable Architecture Search. In *International Conference on Learning Representations*.

[30] Yinhan Liu, Myle Ott, Naman Goyal, Jingfei Du, Mandar Joshi, Danqi Chen, Omer Levy, Mike Lewis, Luke Zettlemoyer, and Veselin Stoyanov. 2019. Roberta: A robustly optimized bert pretraining approach. *arXiv preprint arXiv:1907.11692* (2019).

[31] Renqian Luo, Tao Qin, and Enhong Chen. 2019. Balanced One-shot Neural Architecture Optimization. arXiv:1909.10815 [cs.LG]

[32] Renqian Luo, Xu Tan, Rui Wang, Tao Qin, Enhong Chen, and Tie-Yan Liu. 2020. Neural architecture search with gbdt. *arXiv preprint arXiv:2007.04785* (2020).

[33] J Scott McCarley. 2019. Pruning a bert-based question answering model. *arXiv preprint arXiv:1910.06360* (2019).

[34] Ilija Radosavovic, Raj Prateek Kosaraju, Ross Girshick, Kaiming He, and Piotr Dollár. 2020. Designing network design spaces. In *Proceedings of the IEEE/CVF Conference on Computer Vision and Pattern Recognition*. 10428–10436.

[35] Pranav Rajpurkar, Robin Jia, and Percy Liang. 2018. Know What You Don't Know: Unanswerable Questions for SQuAD. In *Proceedings of the 56th Annual Meeting of the Association for Computational Linguistics (Volume 2: Short Papers)*. 784–789.

[36] Pranav Rajpurkar, Jian Zhang, Konstantin Lopyrev, and Percy Liang. 2016. SQuAD: 100,000+ Questions for Machine Comprehension of Text. In *EMNLP*. 2383–2392.

[37] Victor Sanh, Lysandre Debut, Julien Chaumond, and Thomas Wolf. 2019. DistilBERT, a distilled version of BERT: smaller, faster, cheaper and lighter. *arXiv preprint arXiv:1910.01108* (2019).

[38] Sheng Shen, Zhen Dong, Jiayu Ye, Linjian Ma, Zhewei Yao, Amir Gholami, Michael W Mahoney, and Kurt Keutzer. 2020. Q-BERT: Hessian Based Ultra Low Precision Quantization of BERT.. In *AAAI*. 8815–8821.

[39] Richard Socher, Alex Perelygin, Jean Wu, Jason Chuang, Christopher D. Manning, Andrew Ng, and Christopher Potts. 2013. Recursive Deep Models for Semantic Compositionality Over a Sentiment Treebank. In *EMNLP*. 1631–1642.

[40] Kaitao Song, Hao Sun, Xu Tan, Tao Qin, Jianfeng Lu, Hongzhi Liu, and Tie-Yan Liu. 2020. LightPAFF: A Two-Stage Distillation Framework for Pre-training and Fine-tuning. *arXiv preprint arXiv:2004.12817* (2020).

[41] Siqi Sun, Yu Cheng, Zhe Gan, and Jingjing Liu. 2019. Patient Knowledge Distillation for BERT Model Compression. In *Proceedings of the 2019 Conference on Empirical Methods in Natural Language Processing and the 9th International Joint Conference on Natural Language Processing (EMNLP-IJCNLP)*. 4314–4323.

[42] Zhiqing Sun, Hongkun Yu, Xiaodan Song, Renjie Liu, Yiming Yang, and Denny Zhou. 2020. MobileBERT: a Compact Task-Agnostic BERT for Resource-Limited Devices. In *Proceedings of the 58th Annual Meeting of the Association for Computational Linguistics*. 2158–2170.

[43] Henry Tsai, Jayden Ooi, Chun-Sung Ferng, Hyung Won Chung, and Jason Riesa. 2020. Finding Fast Transformers: One-Shot Neural Architecture Search by Component Composition. *arXiv preprint arXiv:2008.06808* (2020).

[44] Iulia Turc, Ming-Wei Chang, Kenton Lee, and Kristina Toutanova. 2019. Well-read students learn better: On the importance of pre-training compact models. *arXiv preprint arXiv:1908.08962* (2019).

[45] Ashish Vaswani, Noam Shazeer, Niki Parmar, Jakob Uszkoreit, Llion Jones, Aidan N Gomez, Łukasz Kaiser, and Illia Polosukhin. 2017. Attention is all you need. In *Advances in neural information processing systems*. 5998–6008.

[46] Alex Wang, Amanpreet Singh, Julian Michael, Felix Hill, Omer Levy, and Samuel R Bowman. 2018. GLUE: A Multi-Task Benchmark and Analysis Platform for Natural Language Understanding. In *International Conference on Learning Representations*.

[47] Hanrui Wang, Zhanghao Wu, Zhijian Liu, Han Cai, Ligeng Zhu, Chuang Gan, and Song Han. 2020. HAT: Hardware-Aware Transformers for Efficient Natural Language Processing. In *Proceedings of the 58th Annual Meeting of the Association for Computational Linguistics*. 7675–7688.

[48] Linnan Wang, Saining Xie, Teng Li, Rodrigo Fonseca, and Yuandong Tian. 2019. Sample-efficient neural architecture search by learning action space. *arXiv preprint arXiv:1906.06832* (2019).

[49] Wenhui Wang, Furu Wei, Li Dong, Hangbo Bao, Nan Yang, and Ming Zhou. 2020. MiniLM: Deep Self-Attention Distillation for Task-Agnostic Compression of Pre-Trained Transformers. In *Advances in Neural Information Processing Systems 33: Annual Conference on Neural Information Processing Systems 2020, NeurIPS 2020, December 6-12, 2020, virtual*, Hugo Larochelle, Marc'Aurelio Ranzato, Raia Hadsell, Maria-Florina Balcan, and Hsuan-Tien Lin (Eds.). https://proceedings.neurips.cc/paper/2020/hash/3f5ee243547dee91fbd053c1c4a845aa-Abstract.html

[50] Alex Warstadt, Amanpreet Singh, and Samuel Bowman. 2019. Neural Network Acceptability Judgments. *Transactions of the Association for Computational Linguistics* 7 (2019), 625–641.

[51] Adina Williams, Nikita Nangia, and Samuel Bowman. 2018. A Broad-Coverage Challenge Corpus for Sentence Understanding through Inference. In *NAACL*. 1112–1122.

[52] Felix Wu, Angela Fan, Alexei Baevski, Yann Dauphin, and Michael Auli. 2018. Pay Less Attention with Lightweight and Dynamic Convolutions. In *International Conference on Learning Representations*.

[53] Canwen Xu, Wangchunshu Zhou, Tao Ge, Furu Wei, and Ming Zhou. 2020. BERT-of-Theseus: Compressing BERT by Progressive Module Replacing. In *Proceedings of the 2020 Conference on Empirical Methods in Natural Language Processing (EMNLP)*. 7859–7869.

[54] Zhilin Yang, Zihang Dai, Yiming Yang, Jaime Carbonell, Russ R Salakhutdinov, and Quoc V Le. 2019. Xlnet: Generalized autoregressive pretraining for language understanding. In *Advances in neural information processing systems*. 5753–5763.

[55] Jiahui Yu, Pengchong Jin, Hanxiao Liu, Gabriel Bender, Pieter-Jan Kindermans, Mingxing Tan, Thomas Huang, Xiaodan Song, Ruoming Pang, and Quoc Le. 2020. Bignas: Scaling up neural architecture search with big single-stage models. In *European Conference on Computer Vision*. Springer, 702–717.

[56] Ofir Zafrir, Guy Boudoukh, Peter Izsak, and Moshe Wasserblat. 2019. Q8bert: Quantized 8bit bert. *arXiv preprint arXiv:1910.06188* (2019).

A REPRODUCIBILITY

A.1 Operation Set and Search Space

The Design Choice of the Operation Set. In addition to MHA and FFN, LSTM, convolution and variants of MHA and FFN have achieved good performance in many NLP tasks [5, 20, 21]. We describe the considerations to choose the operations as follows: 1) LSTM is not considered due to slow training and inference speed. 2) In our preliminary experiments, we try some variants of MHA and FFN [23, 52], but fail to observe the advantages of small model size and/or better performance. 3) Considering the parameter size of convolution is $K * H^2$ and separable convolution (SepConv) is $H^2 + K * H$ where K and H are the kernel size and hidden size, instead of convolution, we use SepConv with a larger kernel (with a larger receptive field) without significantly increasing the model size and the latency. Based on these considerations, we add SepConv into the candidate operation set.

To determine the possible hidden sizes for operations, we mainly consider the range of the compressed model sizes. Previous works [37, 41] usually compress the pre-trained BERT model into a small model (usually no more than 66M) for efficiency and effectiveness. Similarly, in this work, we aim to obtain compressed models of less than 66M. Therefore, we choose the hidden sizes between 128 and 512 for the candidate operations, which enables a good trade-off between efficiency and effectiveness[3].

The Complexity of the Search Space. The supernet consists of $L = 24$ layers. If we do not use block-wise search, there would be $26^{24} \approx 10^{34}$ paths (possible candidate architectures) in the supernet. We divide the supernet into $N = 4$ blocks and each block contains 6 layers. Within each block, the hidden size of the 6 layers are required to be consistent, and the hidden sizes across different blocks can be different. So there are $5 * 6^6 = 233280$ paths (possible candidate sub-architectures) in each block, where the first 5 is the number of candidate hidden sizes and 6^6 represents that there are 6 operations in 6 layers. Due to the identity operation, there is an unnecessary increase in the possible sequence of operations (architecture) as pointed in Li et al. [25]. For example, the architecture {FFN, identity, FFN, identity} is equivalent to {FFN, FFN, identity, identity}. Thus we only keep the architectures that all of the identity operations are at the end (e.g., {FFN, FFN, identity, identity}) and delete other redundant architectures. After cleaning the redundancy, the search space in each block is reduced from the original 233280 to 97650, which largely improves the sample efficiency. We can select sub-architectures from each block and ensemble them to get a complete model. Considering $N = 4$ blocks, there are 97650^4 (about 10^{20} possible combinations). Therefore the number of possible models is reduced from 10^{34} to 10^{20}.

A.2 Training Configurations

Teacher Model. We train the BERT$_{base}$ (L=12, H=768, A=12) [10] as the teacher model, where L is the number of layers, H is the hidden size, and A is the number of attention heads. Following Devlin et al. [10], we use BookCorpus plus English Wikipedia as pre-training data (16GB in total). We use Adam [22] with a learning rate

---

[3]We do not use a hidden size smaller than 128 since it cannot yield models with enough accuracy.

of 1e-4, $\beta_1 = 0.9$ and $\beta_2 = 0.999$. The learning rate is warmed up to a peak value of 5e-4 for the first 10,000 steps, and then linearly decays. The weight decay is 0.01 and the dropout rate is 0.1. We apply the best practices proposed in Liu et al. [30] to train the BERT$_{base}$ on 16 NVIDIA V100 GPUs with large batches leveraging gradient accumulation (2048 samples per batch) and 125000 training steps.

A.3 Comparison of Teacher Models

We present the performance of the teacher model for reproducibility and compare it with teacher models used in other works in Table 9. The teacher model (IB-BERT) of MobileBERT [42] achieves the performance close to the BERT$_{large}$, which is much better than our teacher model and those used in most related works such as TinyBERT, DynaBERT, DistilBERT. Thus we do not compare NAS-BERT with MobileBERT in Table 3. Except for MobileBERT, other methods use BERT$_{base}$ as the teacher model. Our teacher model is better than others on average, which is mainly caused by the volatility of RTE and CoLA (small dataset). After removing these two datasets, the performance of the teacher model (average score: 89.74) is close to the teacher model of other methods (DistilBERT: 89.73, BERT-of-Theseus: 88.76 and DynaBERT: 89.68). In this way, NAS-BERT can still show its effectiveness compared with other approaches, without considering RTE and CoLA.
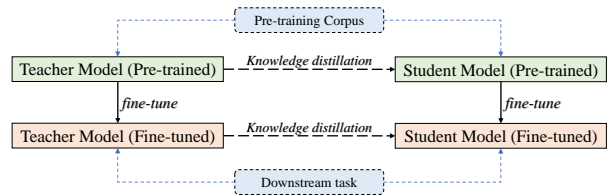

Figure 4: The pipeline of two-stage distillation.

A.4 Two-stage distillation

Two-stage distillation means applying knowledge distillation in both the pre-training and the fine-tuning stage. Previous methods [14, 18, 37, 40] have proved that using two-stage distillation is superior to the single-stage distillation. The pipeline of two-stage distillation is shown in Fig. 4. The procedure of two-stage distillation can be summarized as follows:

(1) Pre-train the teacher model on the pre-training corpus.
(2) Pre-train the light-weight student model with knowledge distillation from the pre-trained teacher model in step 1.
(3) Fine-tune the pre-trained teacher model in step 1 on the downstream task.
(4) Fine-tune the pre-trained student model in step 2 with knowledge distillation from the fine-tuned teacher model in step 3 on the target downstream task.

To simplify our expression, we denote the parameter of the student and the teacher model as θ_S and θ_T respectively. We adopt a general formulation for knowledge distillation in both stages:

$$\mathcal{L}(x, y; \theta_S, \theta_T) = \sum_{(x,y)}^{\{\mathcal{X}, \mathcal{Y}\}} (1 - \lambda) \cdot \mathcal{L}_{MLE}(x, y; \theta_S) \\ + \lambda \cdot \mathcal{L}_{KL}(f(x; \theta_T), f(x; \theta_S)), \tag{2}$$

Table 9: The accuracy of the teacher models on dev set of the GLUE benchmark. IB-BERT* achieves the performance close to the BERT$_{large}$.

Teacher	Method	MNLI-m	QQP	QNLI	CoLA	SST-2	STS-B	RTE	MRPC	AVG
BERT$_{base}$	DistilBERT	86.7	89.6	91.8	56.3	92.7	89.0	69.3	88.6	83.0
	MiNiLM	84.5	91.3	91.7	58.9	93.2	-	68.6	87.3	-
	BERT-of-Theseus	83.5	89.8	91.2	54.3	91.5	88.9	71.1	89.5	82.3
	DynaBERT	84.8	90.9	92.0	58.1	92.9	89.8	71.1	87.7	83.4
	Ours	85.2	91.0	91.3	61.0	92.9	90.3	76.0	87.7	84.4
IB-BERT*	MobileBERT	87.0	-	93.2	-	94.1	-	-	87.3	-

Table 10: Architectures of NAS-BERT. "E", "M", "F" and "S" refer to Embedding, MHA, FFN and SepConv. "S3" refers to SepConv with the kernel size 3. The number in the subscript refers to the hidden size.

Params	Architectures
60M	$E_{512} \to S3_{512} \to M_{512} \to M_{512} \to S7_{512} \to F_{512} \to F_{512} \to F_{512} \to M_{512} \to M_{512} \to S7_{512} \to F_{512} \to F_{512}$ $\to M_{512} \to S5_{512} \to M_{512} \to F_{512} \to S3_{512} \to F_{512} \to M_{512} \to M_{512} \to S5_{512} \to F_{512} \to F_{512} \to F_{512}$
55M	$E_{512} \to F_{512} \to S5_{512} \to M_{512} \to F_{512} \to M_{512} \to F_{512} \to S7_{512} \to M_{512} \to S7_{512} \to M_{512} \to F_{512} \to S5_{512}$ $\to S3_{512} \to M_{512} \to S5_{512} \to S5_{512} \to F_{512} \to F_{512} \to F_{512} \to M_{512} \to M_{512} \to S5_{512} \to F_{512}$
50M	$E_{384} \to F_{512} \to S5_{512} \to M_{512} \to F_{512} \to S5_{512} \to F_{512} \to S7_{512} \to M_{512} \to S7_{512} \to F_{512} \to F_{512} \to S3_{512}$ $\to M_{512} \to S5_{512} \to S7_{512} \to F_{512} \to M_{512} \to F_{512} \to M_{512} \to S5_{512} \to M_{512} \to F_{512}$
45M	$E_{384} \to S3_{512} \to M_{512} \to S7_{512} \to F_{512} \to S5_{512} \to F_{512} \to S7_{512} \to M_{512} \to S7_{512} \to M_{512} \to F_{512} \to S7_{512}$ $\to S3_{512} \to M_{512} \to S7_{512} \to S3_{512} \to F_{512} \to M_{512} \to F_{512} \to M_{512} \to S3_{512} \to S7_{512} \to F_{512}$
40M	$E_{384} \to S3_{512} \to M_{512} \to S5_{512} \to M_{512} \to S5_{512} \to F_{512} \to S5_{512} \to M_{512} \to S7_{512} \to F_{512} \to F_{512} \to S3_{512}$ $\to M_{512} \to S5_{512} \to S5_{512} \to S3_{512} \to F_{512} \to S7_{512} \to M_{512} \to M_{512} \to F_{512}$
35M	$E_{256} \to S3_{512} \to S7_{512} \to M_{512} \to S7_{512} \to S3_{512} \to F_{512} \to M_{512} \to S5_{512} \to S7_{512} \to S5_{512} \to S3_{512} \to M_{512}$ $\to S5_{512} \to S5_{512} \to S3_{512} \to F_{512} \to S7_{512} \to M_{512} \to M_{512} \to F_{512}$
30M	$E_{256} \to S3_{512} \to M_{512} \to S5_{512} \to S7_{512} \to F_{512} \to S5_{512} \to M_{512} \to S7_{512} \to S5_{512} \to F_{512} \to S3_{512} \to S5_{512}$ $\to M_{512} \to F_{512} \to S3_{512} \to S7_{512} \to M_{512} \to S3_{512} \to F_{512} \to S5_{512}$
25M	$E_{256} \to S3_{384} \to M_{384} \to S5_{384} \to S3_{384} \to S3_{384} \to S5_{384} \to S7_{512} \to S5_{512} \to M_{512} \to F_{512} \to F_{512} \to M_{512}$ $\to S_{512} \to M_{512} \to M_{512} \to F_{512}$
20M	$E_{128} \to S3_{384} \to M_{384} \to S5_{384} \to S3_{384} \to S3_{384} \to S5_{384} \to M_{512} \to F_{512} \to F_{512} \to M_{512} \to S3_{384} \to S5_{384}$ $\to M_{384} \to S5_{384} \to S3_{384} \to S5_{384}$
15M	$E_{128} \to S3_{384} \to M_{384} \to S5_{384} \to S3_{384} \to S3_{384} \to S5_{384} \to S5_{384} \to S5_{384} \to M_{384} \to S5_{384} \to S5_{384} \to S7_{384}$ $\to M_{384} \to S5_{384} \to S5_{384} \to S5_{384} \to S5_{384} \to S5_{384} \to S3_{384} \to S5_{384} \to M_{384} \to S5_{384} \to S3_{384} \to S5_{384}$
10M	$E_{128} \to S3_{384} \to S5_{384} \to M_{384} \to S3_{384} \to S5_{384} \to M_{384} \to S7_{384} \to M_{384} \to S3_{384} \to S7_{384} \to M_{384} \to S3_{384}$
5M	$E_{64} \to S3_{192} \to S7_{192} \to M_{192} \to S7_{192} \to S7_{192} \to M_{192} \to S3_{192} \to M_{192} \to S7_{192} \to S5_{192} \to M_{192} \to S3_{192}$

where $\mathcal{L}_{MLE}$ is the maximal likelihood loss of the student model θ_S over the training corpus $(\mathcal{X}, \mathcal{Y})$ (i.e., masked language model loss on the pre-training stage or classification/regression loss on the fine-tuning stage), and $\mathcal{L}_{KL}$ is the KL divergence between the predicted probability distribution $f(x; \theta_T)$ of the teacher model θ_T and the distribution $f(x; \theta_S)$ of the student model θ_S. λ is a hyper-parameter to trade off $\mathcal{L}_{MLE}$ and $\mathcal{L}_{KL}$, and is set as 0.5 in our experiments. There are other advanced distillation techniques (e.g., embedding distillation or attention distillation) but here we only consider prediction layer distillation.

A.5 Architectures of NAS-BERT

Our NAS-BERT can generate different compressed models given specific constraints, as described in Section 3.3. Besides the several NAS-BERT models we evaluate in Table 2, we further select architectures with various sizes, from 5M to 60M with 5M intervals, yielding a total of 12 different architectures with different sizes. We present the architectures in Table 10.